Nanoscale

SUPPLEMENTARY INFORMATION

Wafer-scale fabrication of high-quality tunable gold nanogap arrays for surface-enhanced Raman scattering

Hai Le-The,*†[a] Jasper J. A. Lozeman,†[a] Marta Lafuente,[b] Pablo Muñoz,[c] Johan G. Bomer,[a] Hien Duy-Tong,[d] Erwin Berenschot,[e] Albert van den Berg,[a] Niels R. Tas,[e] Mathieu Odijk,[a] Jan C. T. Eijkel[a]

SI1. Uniformity measurement of fabricated PR and BARC nanoline arrays

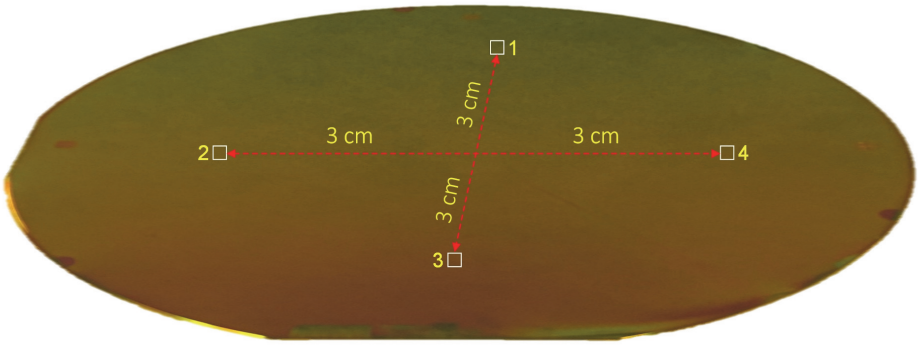

Fig. S1 A wafer-scale array of PR nanolines patterned on an oxidized Si wafer. Four areas indicated by white squares were selected for the uniformity measurement of the fabricated PR nanolines.

[a] *BIOS Lab-on-a-Chip Group, MESA+ Institute, Max Planck Center for Complex Fluid Dynamics, University of Twente, 7522 NB Enschede, The Netherlands. E-mail: h.lethe@utwente.nl*
[b] *Nanoscience Institute of Aragon, Department of Chemical & Environmental Engineering, University of Zaragoza, 50018 Zaragoza, Spain*
[c] *Optical Sciences Group, MESA+ Institute, University of Twente, 7522 NB Enschede, The Netherlands*
[d] *Faculty of Engineering, Vietnamese German University, Thu Dau Mot City, Binh Duong Province, Vietnam.*
[e] *Mesoscale Chemical Systems Group, MESA+ Institute, University of Twente, 7522 NB Enschede, The Netherlands*
† Equal contribution

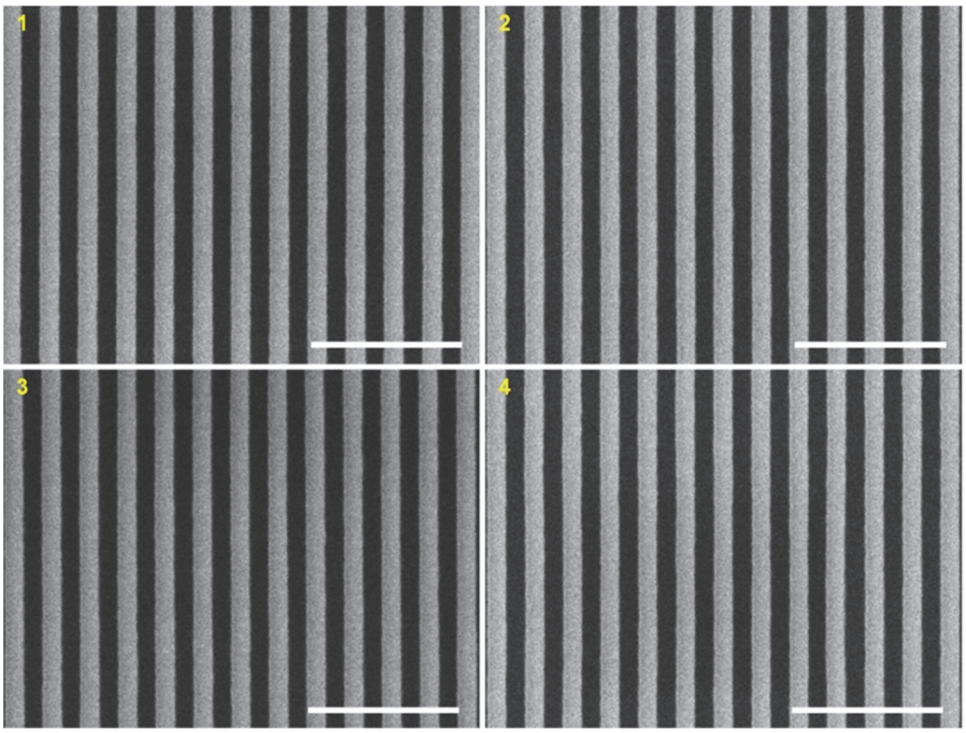

Fig. S2 Top-view HR-SEM images of the fabricated PR nanolines at the four selected areas (see Fig. S1). Scale bars represent 1 µm.

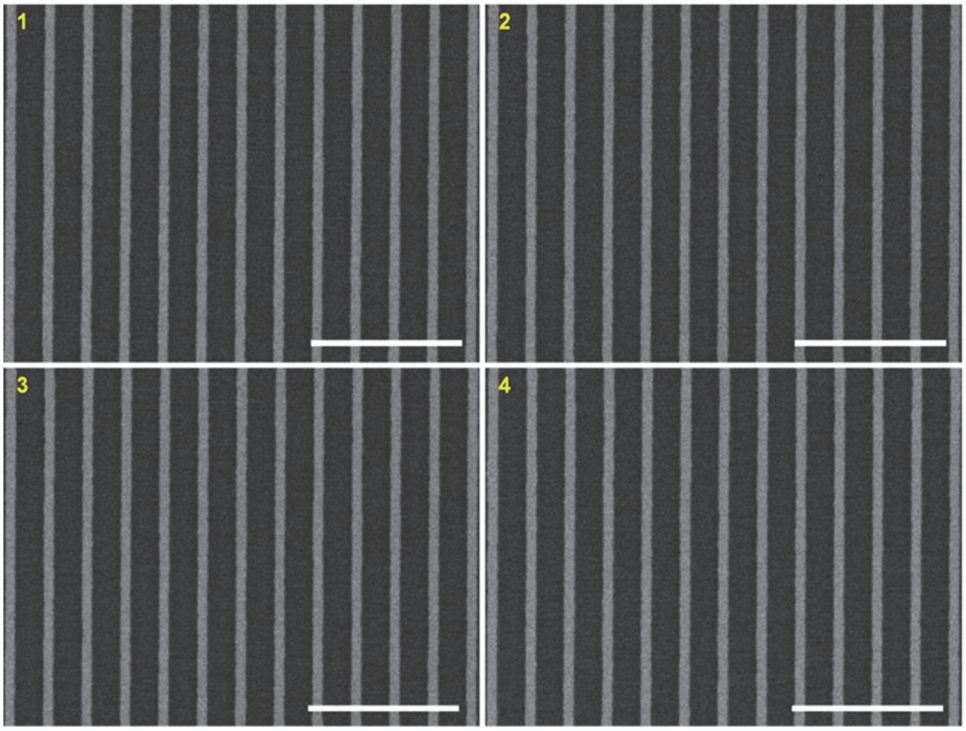

Fig. S3 Top-view HR-SEM images of the fabricated BARC nanolines at the four selected areas (see Fig. S1). Scale bars represent 1 µm.

SI2. Uniformity measurement of fabricated Cr nanoline arrays

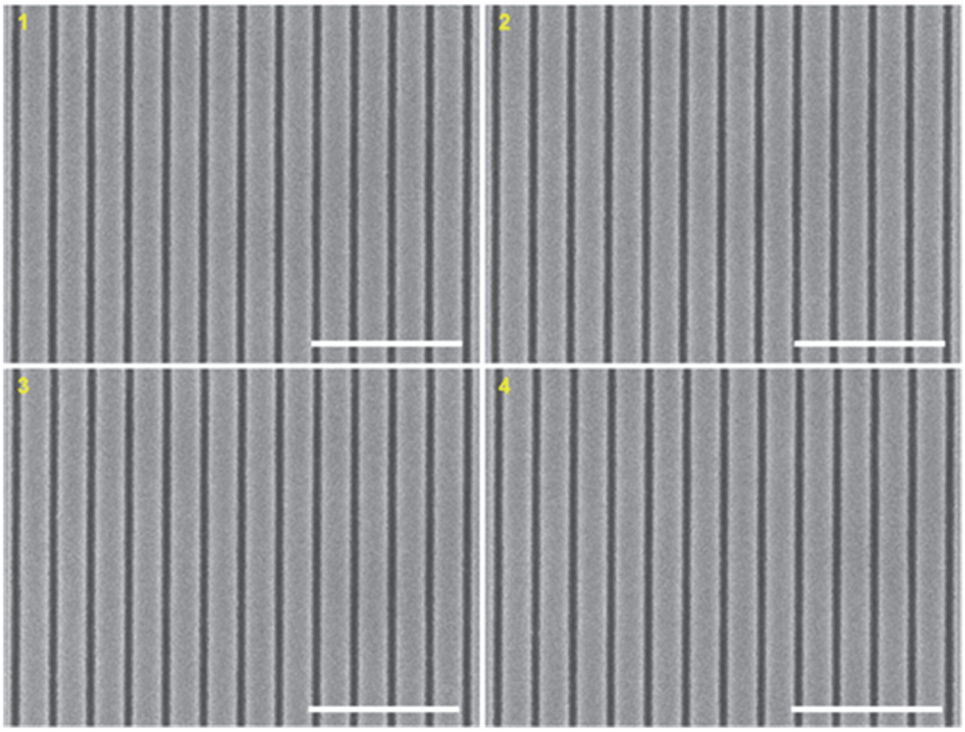

Fig. S4 Top-view HR-SEM images of the fabricated Cr nanolines at the four selected areas (see Fig. S1). Scale bars represent 1 µm.

SI3. Wet etching of bulk Si substrates

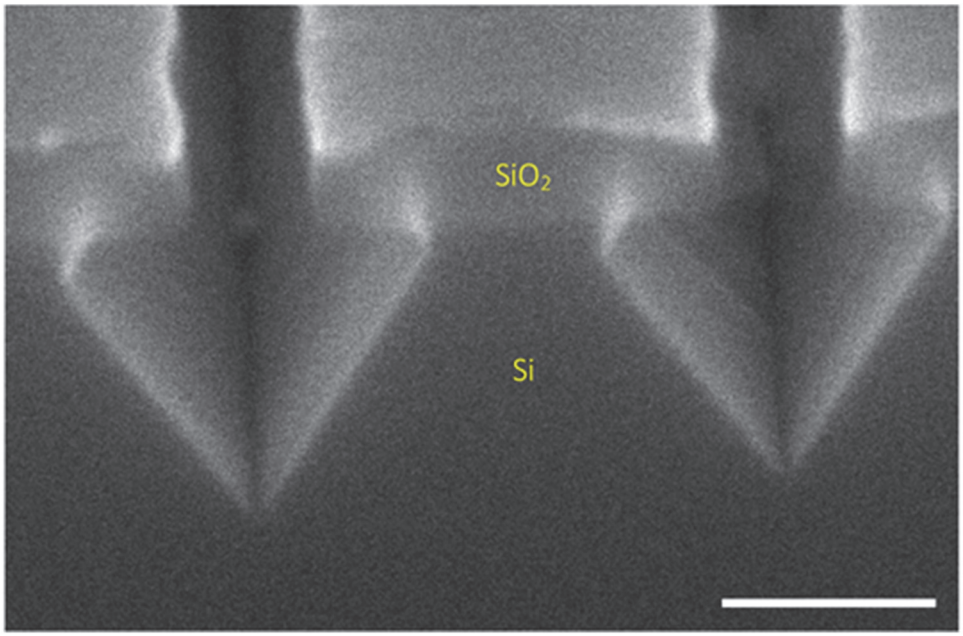

Fig. S5 Cross-sectional HR-SEM image of undesirable v-grooves in bulk Si substrate caused by over etching in the KOH solution. Scale bar represents 100 nm.

SI4. Uniformity measurement of fabricated SiN nanogap arrays

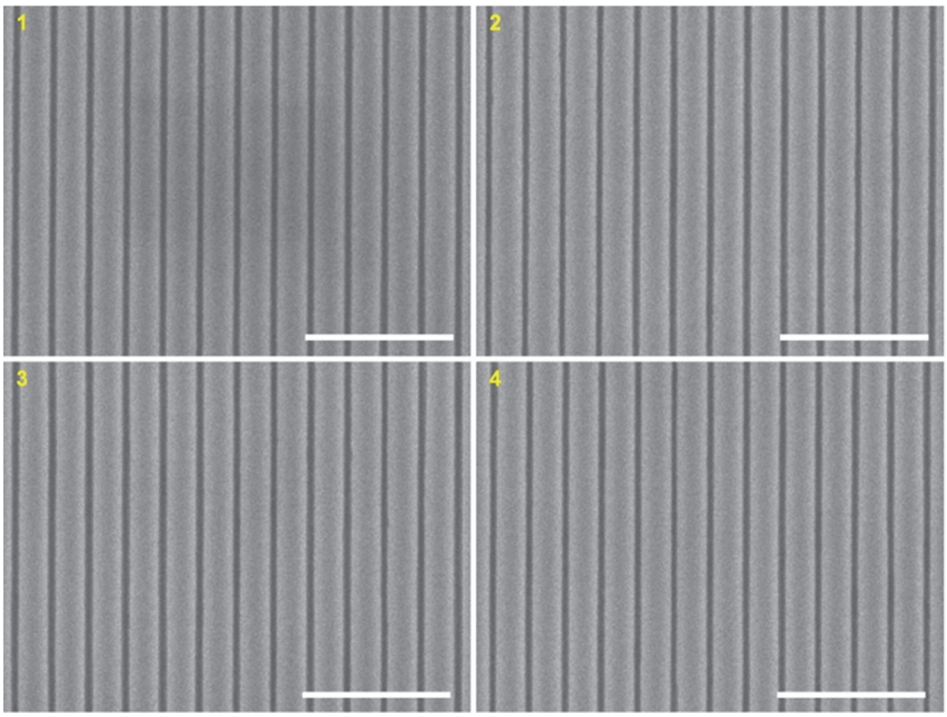

Fig. S6 Top-view HR-SEM images of the fabricated SiN nanogaps at the four selected areas (see Fig. S1). Scale bars represent 1 µm.

SI5. Uniformity measurement of fabricated Au nanogap arrays

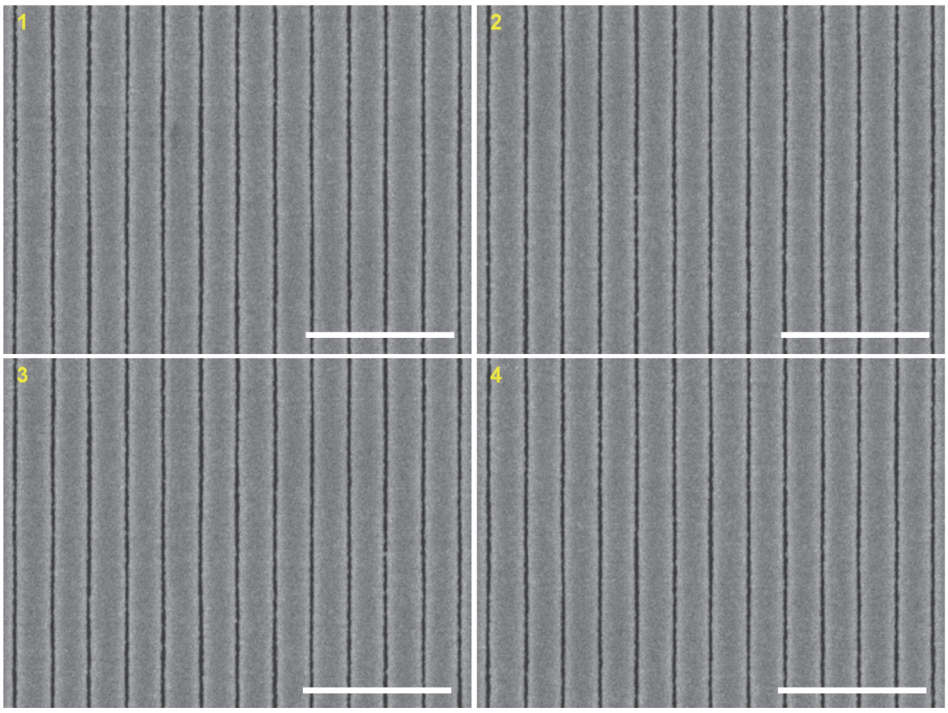

Fig. S7 Top-view HR-SEM images of the fabricated Au nanogaps at the four selected areas (see Fig. S1). Scale bars represent 1 µm.

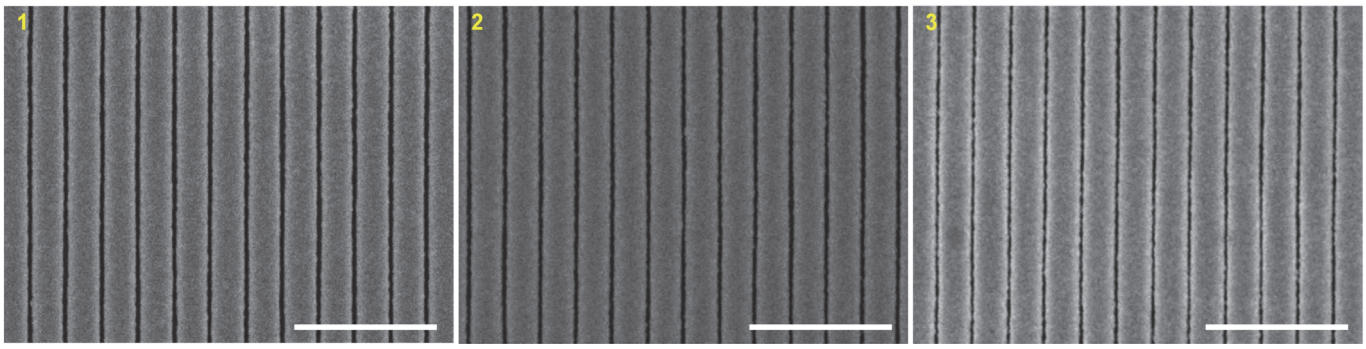

Fig. S8 Top-view HR-SEM images of the Au nanogaps fabricated from three different batches. Scale bars represent 1 µm.

SI6. Surface roughness measurement of sputtered Au layers

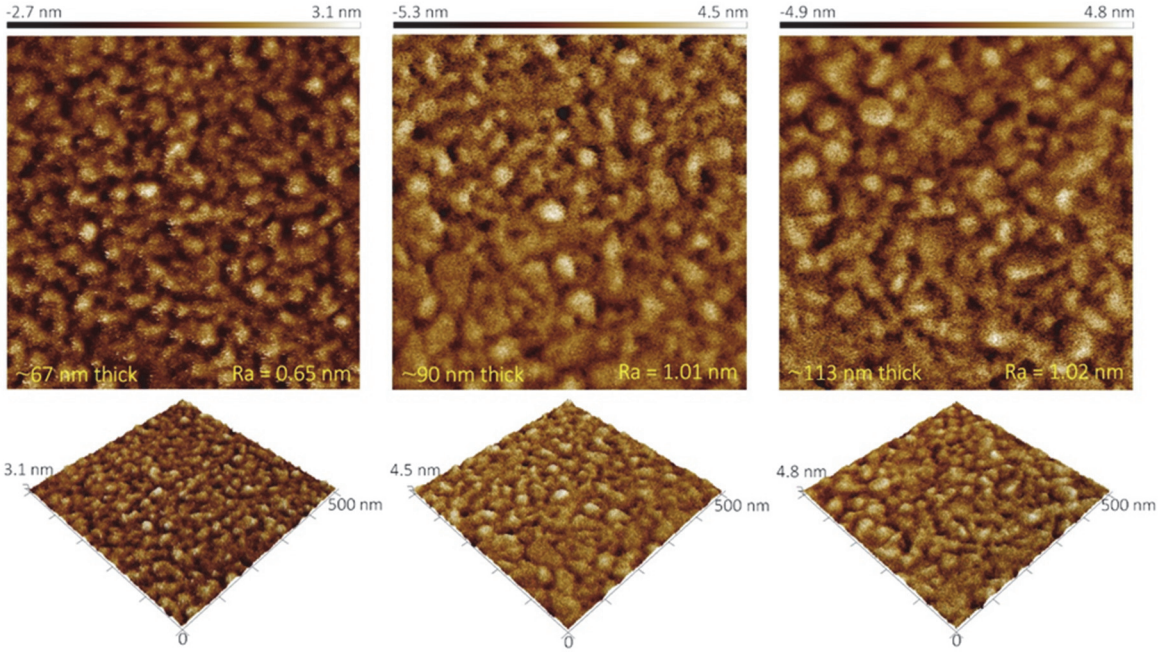

Fig. S9 AFM images (scan field 500×500 nm^2) of Au layers deposited on the surface of oxidized Si wafers at different thicknesses.

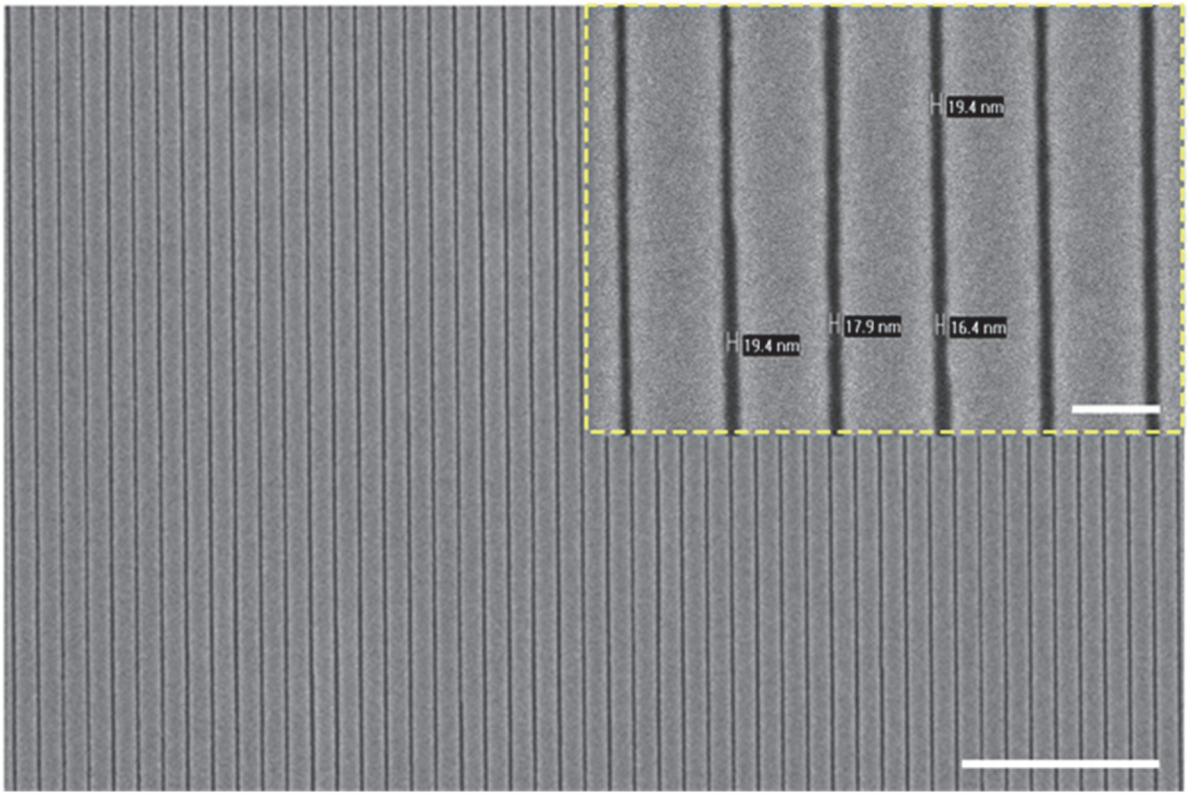

Fig. S10 Top-view HR-SEM image (scale bar 2 µm) of a dense array of sub-20 nm Au nanogaps with a close-up image (scale bar: 200 nm), fabricated by sputtering a Au layer of approximately 90 nm thick over the SiN coated Si template.

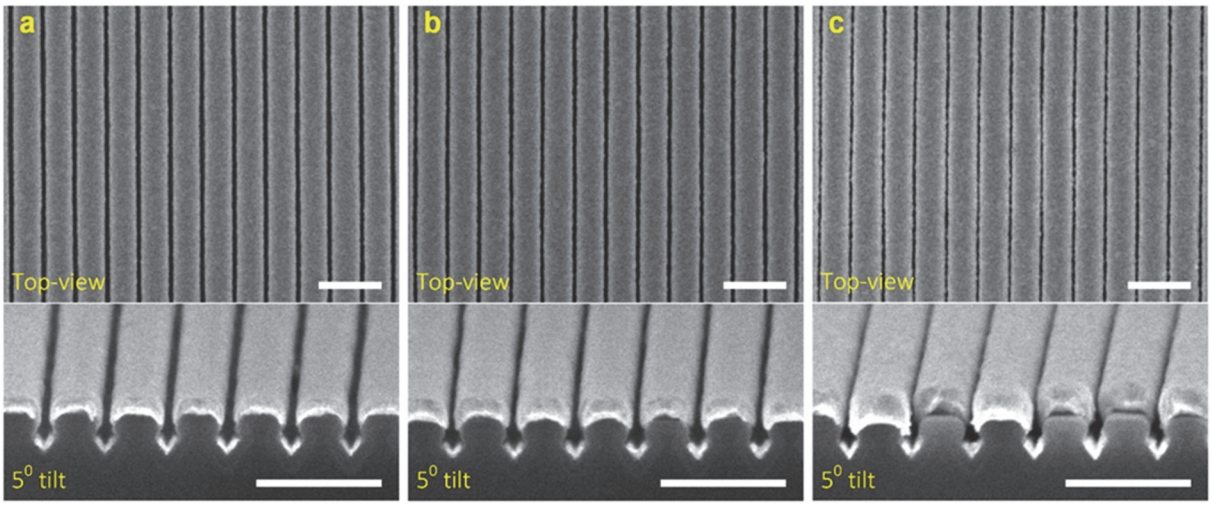

Fig. S11 Top-view and cross-sectional HR-SEM images of the fabricated Au nanogaps with different gap spacings of a) ~30 nm, b) ~20 nm, and c) ~10 nm. Scale bars represent 500 nm.

SI7. Finite-difference time-domain simulations

We estimated the normalized SERS intensity from the local electromagnetic enhancement generated in our Au nanogaps by analyzing the near-field distributions at 785 nm (excitation) and 852 nm (BT Raman

shift at ~999 cm^{-1}) wavelengths (see Fig. S12). The normalized SERS intensity – SERS intensity enhancement – was calculated as follows:[1]

$$Normalized\ SERS\ intensity = \frac{|E|^2_{785nm} \cdot |E|^2_{852nm}}{|E_0|^2_{785nm} \cdot |E_0|^2_{852nm}} \quad \text{(S1)}$$

where $|E|$ is the locally enhanced electric field and $|E_0|$ is the incident electric field calculated for 785 nm, and 852 nm wavelengths.

Due to the exponential decay of the enhanced near field, only the molecules adsorbed on the surface of the SERS structures can show the increased Raman scattering intensity. Therefore, we calculated the expected normalized SERS intensity from only a monolayer of BT covered completely the surface of our Au nanogaps (white lines in Fig. S12). The thickness of a BT monolayer coated on a Au surface was estimated using Materials Studio software (Accelrys Inc., United States), which is approximately 0.8 nm. The SERS-enhanced intensities integrated over the thickness of the considered BT monolayer were 4.1×10^6, 8.2×10^6, and 2.3×10^7 for Au nanogaps of ~30 nm, ~20 nm, and ~10 nm, respectively (Fig. S13). This indicated that although there was a considerable increase in the enhanced electric field in the simulated gap region, only a relatively small increase in the calculated SERS intensities due to the presence of a BT monolayer.

Despite of the fact that the simulations proved to be useful for understanding the origin of the behavior differences of our Au nanogaps of different gap spacings – the simulations follow the expected trend from the experimental measurements – no absolute comparison between the calculated SERS intensity and the measured SERS intensity is intended. Because the simulations were performed using a two-dimensional model, which was simplified from the three-dimensional structure of the fabricated Au nanogaps.

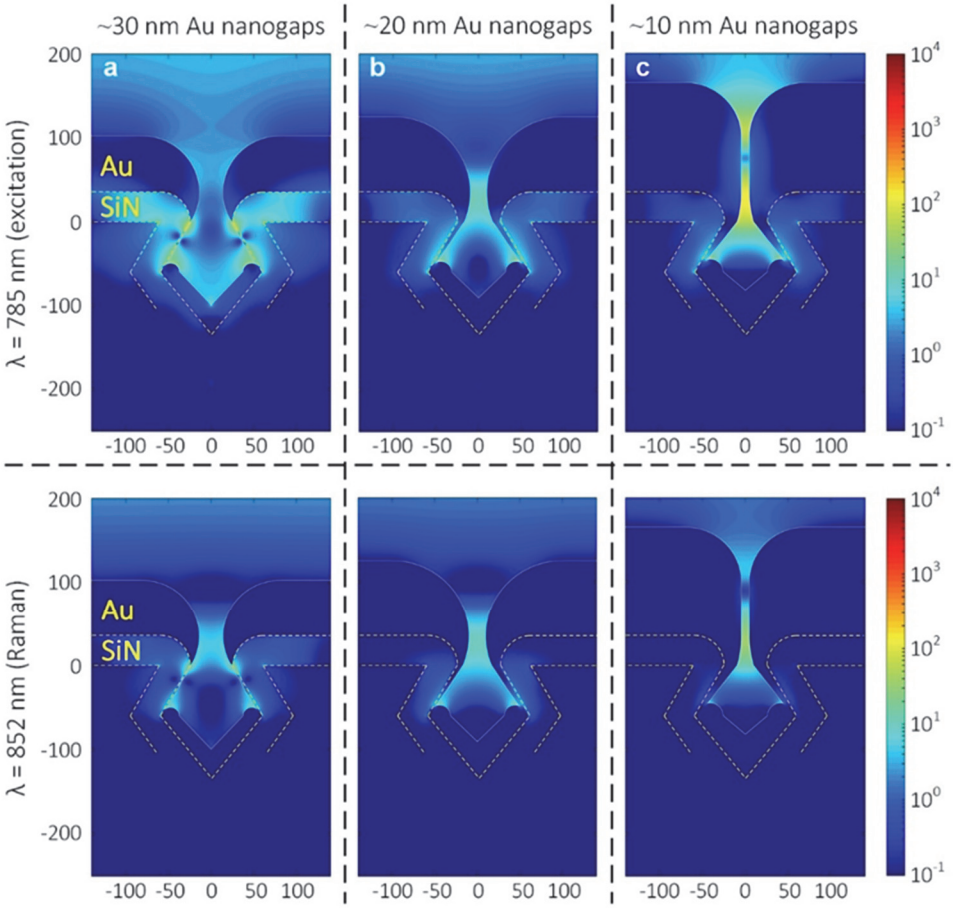

Fig. S12 FDTD-simulated distribution of the local field intensity enhancement factor ($|E|^2/|E_0|^2$) for Au nanogaps of a) ~30 nm, b) ~20 nm, and c) ~10 nm at excitation (785 nm) and Raman (852 nm or 999cm^{-1}) wavelengths. The yellow dashed lines indicate the SiN boundary, whereas the white lines on the Au surface indicate the BT monolayer.

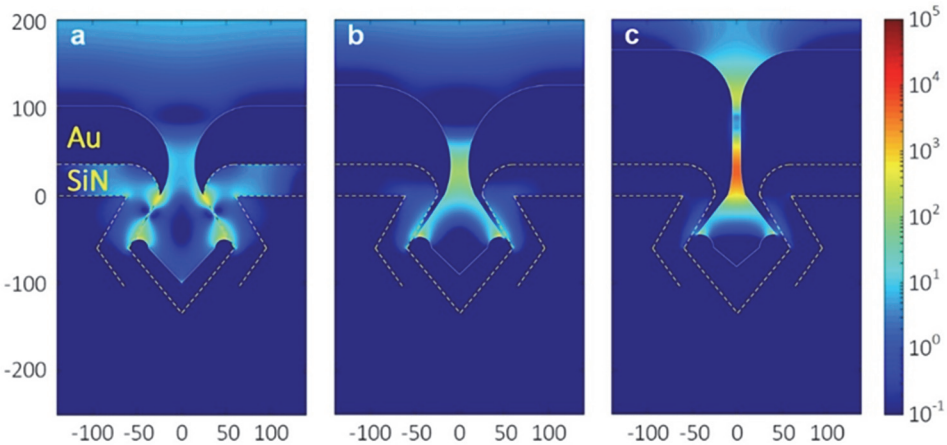

Fig. S13 FDTD-simulated distribution of the SERS intensity ($|E|^4$) for Au nanogaps of a) ~30 nm, b) ~20 nm, and c) ~10 nm. The yellow dashed lines indicate the SiN boundary, whereas the white lines on the Au surface indicate the BT monolayer.

SI8. Surface-enhanced Raman scattering measurements

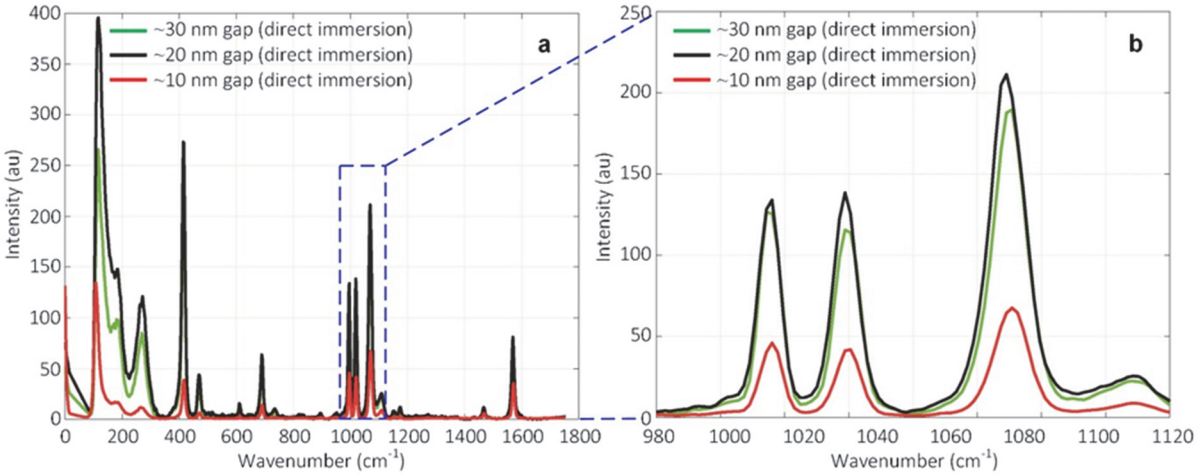

Fig. S14 SERS signals measured on Au nanogaps of ~30 nm, ~20 nm, and ~10 nm gap spacing. All the Au nanogaps were immediately immersed into the BT solution, parallel to the solution surface.

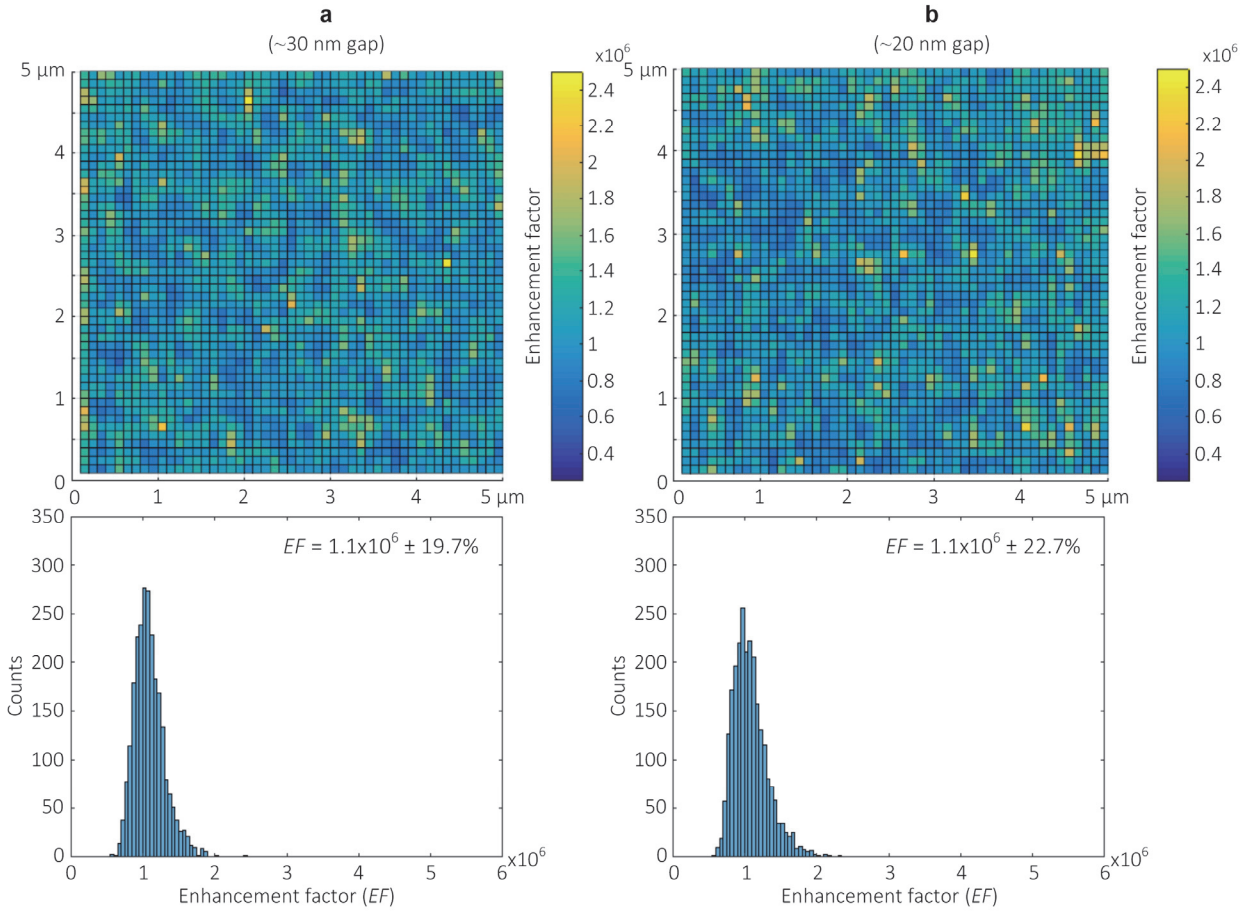

Fig. S15 Calculated enhancement factors and the corresponding histogram of the obtained spectra over a 5×5 µm^2 area for Au nanogaps of a) ~30 nm and b) ~20 nm.

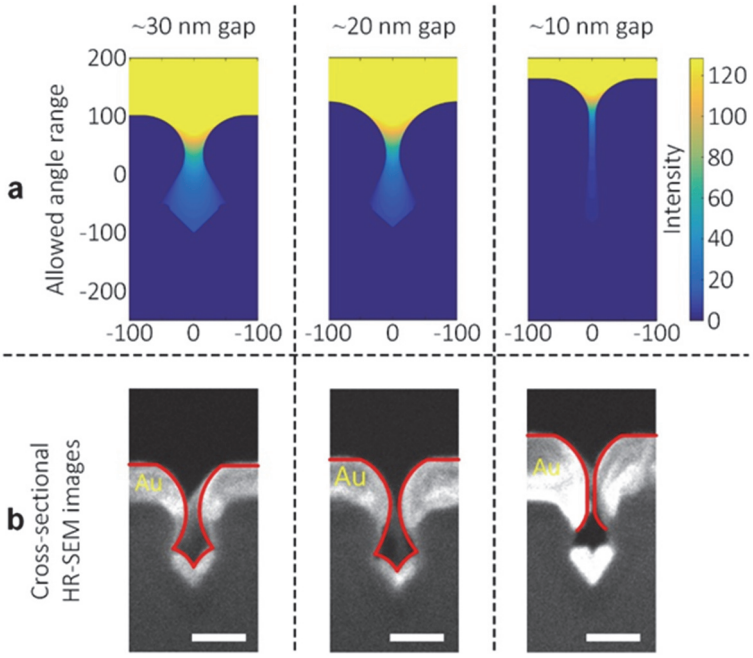

Fig. S16 a) Simulation of the allowed angle range of our fabricated Au nanogaps. b) Estimation of the reachable surface of the Au nanogaps (red lines). It is worth noting that in case of ~10 nm gaps the scattering signal from the cavity under the gap may not reach to the detector. Therefore, the surface of this cavity did not consider in the totally estimated surface. Scale bars represent 100 nm.

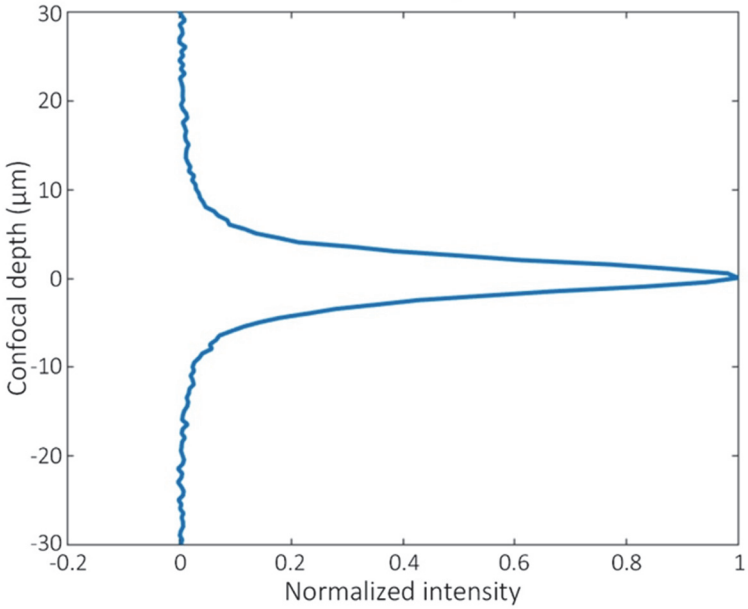

Fig. S17 Normalized collection efficiency.

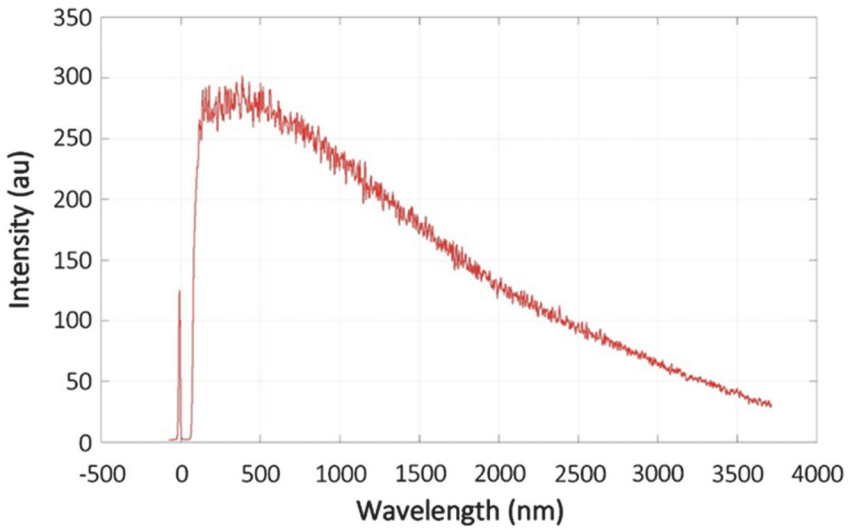

Fig. S18 SERS signal of ~10 nm Au nanogap array with an excitation laser of 525 nm. High fluorescence background is visible, but no signal of BT is observed (2500 scan average).

References

1 E. C. L. Ru and P. G. Etchegoin, Elsevier, 2009, 185-264.